Remote Sensing of Environment 113 (2009) 1012–1024

Contents lists available at ScienceDirect

Remote Sensing of Environment

journal homepage: www.elsevier.com/locate/rse

The CM-SAF operational scheme for the satellite based retrieval of solar surface irradiance — A LUT based eigenvector hybrid approach

R.W. Mueller [a,*], C. Matsoukas [b], A. Gratzki [a], H.D. Behr [a], R. Hollmann [a]

[a] *Climate Monitoring Satellite Application Facility, German Meteorological Service, Germany*
[b] *Department of Environment, University of the Aegean, Greece*

ARTICLE INFO

Article history:
Received 25 March 2008
Received in revised form 20 January 2009
Accepted 24 January 2009

Keywords:
Solar surface irradiance
Radiative transfer modelling
Interactions with atmosphere (clouds, aerosols, water vapour) and land/sea surface
Remote sensing

ABSTRACT

The radiation budget at the earth surface is an essential climate variable for climate monitoring and analysis as well as for verification of climate model output and reanalysis data. Accurate solar surface irradiance data is a prerequisite for an accurate estimation of the radiation budget and for an efficient planning and operation of solar energy systems.

This paper describes a new approach for the retrieval of the solar surface irradiance from satellite data. The method is based on radiative transfer modelling and enables the use of extended information about the atmospheric state. Accurate analysis of the interaction between the atmosphere, surface albedo, transmission and the top of atmosphere albedo has been the basis for the new method, characterised by a combination of parameterisations and "eigenvector" look-up tables. The method is characterised by a high computing performance combined with a high accuracy. The performed validation shows that the mean absolute deviation is of the same magnitude as the confidence level of the BSRN (Baseline Surface Radiation Measurement) ground based measurements and significant lower as the CM-SAF (Climate Monitoring Satellite Application Facility) target accuracy of 10 W/m^2. The mean absolute difference between monthly means of ground measurements and satellite based solar surface irradiance is 5 W/m^2 with a mean bias deviation of −1 W/m^2 and a RMSD (Root Mean Square Deviation) of 5.4 W/m^2 for the investigated European sites. The results for the investigated African sites obtained by comparing instantaneous values are also encouraging. The mean absolute difference is with 2.8% even lower as for the European sites being 3.9%, but the mean bias deviation is with −1.1% slightly higher as for the European sites, being 0.8%. Validation results over the ocean in the Mediterranean Sea using shipboard data complete the validation. The mean bias is −3.6 W/m^2 and 2.3% respectively. The slightly higher mean bias deviation over ocean is at least partly resulting from inherent differences due to the movement of the ship (shadowing, allocation of satellite pixel). The validation results demonstrate that the high accuracy of the surface solar irradiance is given in different climate regions. The discussed method has also the potential to improve the treatment of radiation processes in climate and Numerical Weather Prediction (NWP) models, because of the high accuracy combined with a high computing speed.

1. Introduction

The radiation budget at the Earth's surface is a key parameter for climate monitoring and analysis. It describes part of the energy fluxes between the surface and the atmosphere. Negative or positive values of the radiation budget are compensated by heat fluxes, which in turn cause small and large scale atmospheric motions. On the other hand the radiation budget is determined by atmospheric and surface properties. These interactions play an important role in climate research. Satellite data allow the determination of the radiation budget with a high resolution in space–time and a large regional coverage (up to global) by a combination of different satellites. Satellites provide, through their instruments, information on the interaction of the atmospheric state and the Earths surface with the incoming solar radiation. This information is the basis for the retrieval of radiation products.

Radiation products with a large geographical coverage and a high resolution in space–time are necessary for a better understanding of climate variability, climate dynamics (extremes and the change of patterns in space–time) and for assessing the radiative forcing of the climate system. Moreover, these data are well suitable for the verification of reanalysis data and regional climate models, e.g. Babst et al. (2008). Finally, climate indices derived from satellite based products are of value for monitoring and seasonal prediction of specific climate impacts, e.g. Wang and Qu (2007).

One of the radiation budget components, the solar surface irradiance, is also necessary for an efficient planning and monitoring of solar energy systems. Furthermore it is of importance for the satellite based estimation of drought and evaporation. Solar surface irradiance assessment from geostationary satellites constitutes a

* Corresponding author.
E-mail address: richard.mueller@dwd.de (R.W. Mueller).

0034-4257/$ – see front matter © 2009 Elsevier Inc. All rights reserved.
doi:10.1016/j.rse.2009.01.012

powerful alternative to meteorological ground network for climatological data (Perez et al., 1998a) and is the primary source of information in regions where ground based measurements are sparse (e.g. Ocean, Africa).

The solar surface irradiance retrieval reported in this paper is part of a suite of products derived within the Satellite Application Facility on Climate Monitoring (CM-SAF)[1]. The CM-SAF is part of the European Organisation for the Exploitation of Meteorological Satellites (EUMETSAT) ground segment and part of the EUMETSAT network of Satellite Application Facilities (Schmetz et al., 2002). It contributes to the operational long term monitoring of the climate system by providing Essential Climate Variables (GCOS, 2003) related to the energy and water cycle of the atmosphere. These are currently cloud parameters, surface and top of atmosphere (TOA) radiation budget components and atmospheric water vapour (Woick et al., 2002).

The CM-SAF solar surface irradiance retrieval is based on radiative transfer calculations using satellite-derived parameters as input. In the context of the CM-SAF it is applied to data from the Spinning Enhanced Visible and Infrared Imager (SEVIRI) and Geostationary Earth Radiation Budget (GERB) instruments on-board the European operational weather satellite Meteosat Second Generation (MSG) and to Advanced Very High Resolution Radiometer (AVHRR) data on-board the National Oceanic and Atmospheric Administration (NOAA) and Meteorological Operational (MetOp) satellites for northern latitudes not covered by the geostationary satellite data.

Different methods exist to derive the solar surface irradiance from satellite data. A first class of methods, mainly used for data from geostationary satellites, uses normalised reflectance measurements to determine the cloud transmission or cloud index. A clear sky model is used afterwards to calculate the solar surface irradiance based on the retrieved cloud index. One example for this type of methods is the Heliosat method (Cano et al., 1986; Hammer et al., 2003). It converts METEOSAT satellite data into irradiance with a accuracy better than that derived from interpolated ground measurements (Perez et al., 1998b, 2001). The Heliosat method has been used to generate cloud index data as basis for the surface solar irradiance and daylight data of the European database Satel-Light, which delivers valuable information to architects and other stakeholders (e.g. solar project managers) (Fontoynont et al., 1997). It has also been used within the SoDa service[2] (Wald et al., 2002) for the calculation of the solar surface irradiance. There exist also several derivatives of Heliosat, e.g. Heliosat-2 (Rigolier et al., 2004) which is optimised as an operational processing chain for climatological data (HelioClim). Heliosat and derivatives are also the basis for the SOLEMI service (Solar Energy Mining, www.solemi.de (Meyer et al., 2003)) and the ESA Envisolar project (Environmental Information Services for Solar Energy Industries, www.envisolar.com).

A similar method for Meteosat First Generation data was developed by Möser and Raschke (1984), which is routinely applied at the German Weather Service (Diekmann et al., 1988). A similar method is also used for the GEWEX Surface Radiation Budget project as a quality control algorithm (Gupta et al., 2001; Darnell et al., 1992). This algorithm known as Staylor algorithm is one of the two chosen by the World Climate Research Program (WCRP) SRB project for generating surface solar irradiance for the period March 1985 through December 1998. The results of this algorithm compared well with ground based measurements (Whitlock et al., 1995) and have been used to produce a short-wave data set covering the 12-year period July 1983 through June 1995. In the meantime the SRB data set has been extended to June 2005.

Another type of method relates top of atmosphere reflected radiation flux density to the solar irradiance at the surface. One prominent and widely used approach in this class is the method of Pinker and Lazlo, which uses look-up tables for the retrieval of solar surface irradiance (Pinker & Laszlo, 1992). The parameters in the GEWEX (Global Energy and Water Cycle Experiment) short-wave data set were generated using the Pinker/Laszlo short-wave algorithm. This approach has also been the basis for the first operational version (hereafter) referred as prototype of the CM-SAF scheme, described and validated in Hollmann et al. (2006) and Hollmann and Gratzki (2003). The prototype however differs relative to Pinker and Lazlo in the used input data and the atmospheric processes covered by the used pre-calculated look-up tables (LUTs).

A different type of approach uses retrieved cloud microphysical information in order to derive the solar surface irradiance I. For example, Deneke and Feijt (2008) use information of cloud physical properties retrieved with a LUT approach for the estimation of surface solar irradiance. The retrieval of the cloud physical properties has been developed by the Royal Netherlands Meteorological Institute (KNMI) and is used operationally to provide cloud optical thickness, liquid water path and particle size from satellite imagers within the CM-SAF (Roebeling et al., 2005).

Another example for a SIS retrieval is the method of Bishop and Rossow (1991). They developed a fast radiative transfer algorithm for calculating the surface solar irradiance which uses the total cloud amount and cloud optical depth from the International Satellite Cloud Climatology Project (ISCCP) as important input parameters. The ISCCP method for cloud detection is described in Rossow and Garder (1993). Respective data is available from ISCCP web page and as Surface Solar Irradiance data set from NASA GISS.

The reasons for the development of new generations of RTM based algorithms dedicated for operational processing is discussed in detail in Mueller et al. (2004). The main motivation is that RTM based retrieval algorithms have the potential to exploit the increased information on the atmospheric state, ranging from new satellite systems to improvements in numerical weather prediction (NWP) analysis data. Yet, for operational processing a high computing performance of the algorithm is a pre-requisite.

The solar surface irradiance as well as the outgoing flux density at the top of atmosphere can be derived from the transmission and the top of atmosphere albedo respectively, using the incoming solar irradiance at the top of atmosphere, which is routinely observed. Hence throughout the paper the transmission is equivalent to the solar surface irradiance and the top of atmosphere (TOA) to the outgoing solar flux density (at TOA) in terms of the applicability of the methods and parameterisations.

1.1. Principle of the look-up table (LUT) approach

The surface solar irradiance (I) is defined as the incoming solar radiation at the surface in the 0.2–4.0 µm wavelength region. The scheme applied to retrieve the solar irradiance at the surface is based on Radiative Transfer Model (RTM) calculations, following a lookup table approach. A lookup table (LUT) is a data structure, used to replace a runtime computation with a simpler interpolation operation within discrete pre-computed results.

In our case pre-computed RTM results contain the transmittance — for cloudy situations the relation between transmittance and the top of atmosphere albedo — for a variety of atmospheric and surface states. Once the LUTs have been computed, the transmittance for a given atmospheric state can be extracted from the LUTs by interpolation for each satellite pixel and time. Finally, solar surface irradiance can be calculated from the transmittance by multiplication with the extraterrestrial incoming solar flux density.

The idea behind the LUT approach for an irradiance retrieval scheme is to get equal results as with the direct usage of an RTM, but without the need to perform RTM calculations for each pixel and time, thus leading to an improved computing performance.

In order to generate the look-up tables for the CM-SAF prototype algorithm (first version) RTM calculations of the look-up tables were

[1] (www.cmsaf.eu).
[2] Integration and exploitation of networked Solar radiation Databases for environment monitoring project.

done for a wide range of values for water vapour, ozone, aerosol optical thickness and surface albedo. Several aerosol types were included (Hess et al., 1998). Water clouds were placed at a fixed altitude as a plan-parallel layer and calculations were done with a range of values for the effective radius and the cloud optical thickness.

In cloudy situations, the operational computation of the surface irradiance involves two steps. First the broadband TOA albedo is determined from the satellite measurement (e.g. GERB, Geostationary Earth Radiation Budget). Then the atmospheric transmittance is determined from the pre-computed look-up tables (LUTs) using the TOA albedo together with information on the atmospheric state and surface albedo. For clear sky situations the transmittance is directly determined from the look-up tables without the use of the top of atmosphere albedo, for reasons discussed in more detail in the next section. This leads to a separate LUT for cloudy and clear sky situations.

Needed input data, like the broadband TOA albedo, the surface albedo and the cloud cover are retrieved from satellite data within the CM-SAF. All other input data are either climatological data sets (aerosol, ozone) or NWP analysis data (water vapour). The used input data is discussed in more detail in Section 3.1.

Fig. 1 illustrates the principle of the LUT approach. In this approach, the LUT contains information that relate the surface irradiance to a multitude of quantities, like aerosols, clouds, surface albedo, humidity and temperature profiles, etc. In this work, we will introduce parameterisations and propose methods that will substantially decrease the size of the LUT, as well as its dependence on all the aforementioned quantities. Therefore, the computing speed for the generation of the operational products will be much higher without loss of accuracy.

2. The new scheme

2.1. Introduction into the new concept

Look-up tables work well but they have a significant disadvantage if generated and applied in a pure technical manner, referred hereafter as "pure technical" LUT.

A large number of RTM runs have to be performed in advance for the generation of the LUTs leading to big and cumbersome LUTs. Since recalculation of LUTs can be very time consuming and requires a big effort, the threshold for recalculation is high.

Still, a lot of operational processing time is needed due to interpolation within large multi-dimensional arrays. These limitations can be overcome by reducing the needed amount of RTM calculations as much as possible. Optimisation of the computing performance is quite important, because of the large amount of pixels that have to be processed. In this context the

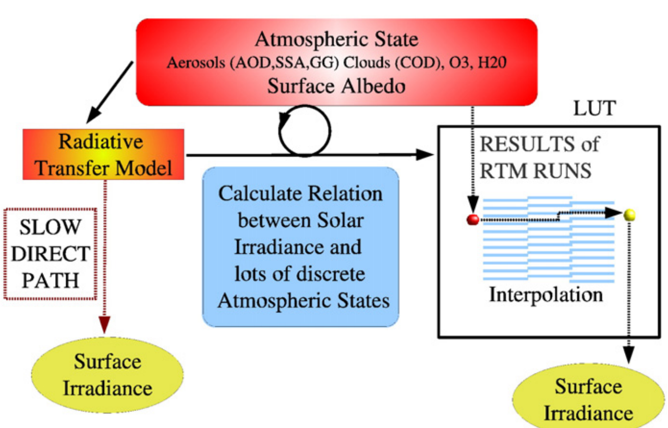

Fig. 1. The principle of a LUT approach. The relation of the transmission to a manifold of atmospheric states is pre-calculated with a radiative transfer model (RTM) and saved in a look-up table (LUT). Based on the amount of considered atmospheric states the LUT table is large. 10^5 to 10^7 calculations are usually needed for the LUT approach if specific scientific optimisations are not applied.

design of a LUT algorithm is always faced with the question on how to reach a high computing speed without loosing significant accuracy.

Reducing computing time is especially important for the reprocessing of large amounts of satellite data (in the order of several years to a few decades) to produce high-quality homogeneous time series suitable for climate monitoring purposes.

In order to minimise the RTM runs needed to describe the interaction between the atmospheric state, the surface albedo and the surface solar irradiance (transmittance), the symmetries and principal components of the relation between the atmospheric transmission and state have been analysed, leading to the following changes relative to the original CM-SAF prototype algorithm.

- Parameters with marginal effect on I (<0.1%) have been left out.
- The interpolation grid has been optimised by reducing the mesh points as much as possible, taking into account the effect of the parameters on the atmospheric transmission in combination with its degree of non-linearity. For example, for a parameter with large effect on the atmospheric transmission but a predominantly linear behaviour the interpolation grid can be wide-meshed, while with increasing non-linearity the distance between the grid-points has to be decreased.
- Inherent symmetries of the relation between the atmospheric state and transmission have been evaluated in order to define a basis system characterised by processes which can be treated as linearly independent on each other. In mathematical terms a basis coordinate system has been evaluated. For the linearly independent parameter set a "pure technical" LUT with (an) optimised interpolation grid has been calculated. For the processes which can be treated as linearly dependent on the basis coordinate system parameterisations have been developed and applied in order to consider their effect on the solar surface irradiance. This approach is referred to be a "eigenvector" approach and is discussed in more detail in Section 2.2.

The goal of the process has been the development of a new scheme which is characterised by high flexibility and accuracy combined with high computing performance. The amount of needed RTM calculations for LUTs can be reduced by several orders of magnitude.

The development of the LUT approach discussed hereafter is based on extensive sensitivity studies performed and documented within visiting scientist studies (e.g. "RTM Calculations for Surface Incoming Shortwave Radiation" by J. Gimeno-Ferrer and R. Hollmann) as well as within the scientific prototype report (Hollmann & Gratzki, 2003). The respective reports are available at the CM-SAF web page.[3] More over, it is based on sensitivity studies performed within the European Heliosat-3 project and recent RTM runs performed for the development of the improved LUT approach. These sensitivity studies have been supported and complemented by studies of other authors, e.g. Li et al. (1993).

In the new CM-SAF algorithm MAGIC (Mesoscale Atmospheric Global Irradiance Code) two look-up tables are used, one for clear sky and one for cloudy sky. The separate treatment of clear sky and cloudy sky situations is motivated by the fact that clear and cloudy sky situations are quite different with regard to the needed interpolation grid and the dominant physical processes. Especially the effect of the surface albedo on the top of atmosphere albedo is much higher than it is for the transmission. Hence, separate LUTs enable the optimisation of the LUT algorithm. Additionally, this concept provided a stand alone clear sky model, which can also be used to improve the computing performance of the SOLIS/Heliosat method. The RTM model libRadtran (Mayer and Kylling, 2005) has been used for the computation of the LUTs and the analysis of the interaction between radiation and the atmosphere. libRadtran is a collection of C and Fortran functions and programs for calculation of solar and thermal radiation in the Earth's atmosphere (A. Kylling and B. Mayer, http://www.libradtran.org). It

[3] (www.cmsaf.eu, Documentation).

has also been validated by comparison with other radiative transfer models (Koepke et al., 1998; Van Weele et al., 2000), and radiation measurements (Mayer et al., 1997).

2.2. Meaning of eigenvector approach

The pure mathematical definition of eigenvalues and eigenvectors can be extended to any operator H. H might be "rotate by 360 degrees" or "stretch in direction of y-axis" or operators in Quantum theory or in radiative transfer as in our case. In these cases, the concept of direction loses its ordinary meaning, and is given an abstract definition. We write $H(\vec{x})$ to mean 'the action of operator H on vector $\vec{x}$'. $\vec{x}$ might be a particular vector that is rotated or stretched or it might be a quantum state or some other object. A eigenvector of operator H is preserved by the operator H apart from a scalar multiplier k, hence, if for the operator H a vector $\vec{x}$ and a scalar k exist so that the following equation is true:

$$H\left(\vec{x}\right) = k^* \vec{x}$$

then $\vec{x}$ is an eigenvector of operator H. This means that the vector changes only the length but not the "direction" and that this length (absolute value of the vector) is k times bigger than what it was before H acted upon it.

A vector is usually defined within a coordinate system. In our case the vector is defined as $\vec{I}$ the solar surface irradiance with a "direction" and length given by its dependency on the parameters of the atmospheric state and surface albedo for a fixed solar zenith angle. Hence the initial coordinate system is given by the atmospheric state (surface albedo, single scattering albedo, asymmetry factor, water vapour, ozone, surface albedo), referred as Astate in the following formulas.

In our case the operator describes the effect of the radiative transfer model on $\vec{I}$ if a specific atmospheric parameter is varied. For water vapour variations (δH_2O) the following relation is given.

$$\mathrm{RTM}_{\delta \mathrm{H_2O}}\left(\vec{I}_{\mathrm{Astate}}\right) = k \cdot \vec{I}_{\mathrm{Astate}}. \tag{1}$$

As the effect of water vapour is predominantly independent on the underlying atmospheric state only the length but not the "direction" of $\vec{I}_{\mathrm{Astate}}$ is changed if the operator $\mathrm{RTM}_{\delta \mathrm{H_2O}}$ is applied. In other words, k remains always the same number for a given δH_2O independent of atmospheric state. Hence, $\vec{I}_{\mathrm{Astate}}$ can be referred as an eigenvector related to the operator $\mathrm{RTM}_{\delta \mathrm{H_2O}}$ (also true for the operator $\mathrm{RTM}_{\delta \mathrm{O_3}}$ and $\mathrm{RTM}_{\delta \mathrm{SAL}}$).

This is not the case for the operator $\mathrm{RTM}_{\delta \mathrm{AOD}}$, $\mathrm{RTM}_{\delta \mathrm{ssa}}$ or $\mathrm{RTM}_{\delta \mathrm{gg}}$, belonging to the effect of variations in the aerosol optical depth, the single scattering albedo and the asymmetry parameter on $\vec{I}_{\mathrm{Astate}}$, respectively. In descriptive terms the $\vec{I}_{\mathrm{Astate}}$ vector does change the length and the "direction" concerning the application of operator $\mathrm{RTM}_{\delta \mathrm{AOD}}$, $\mathrm{RTM}_{\delta \mathrm{ssa}}$, $\mathrm{RTM}_{\delta \mathrm{gg}}$. k is variable and depends on atmospheric state for a given δAOD (also true for δssa and δgg).

As $\vec{I}$ can be referred as an eigenvector concerning the operator $\mathrm{RTM}_{\delta \mathrm{H_2O}}$ and $\mathrm{RTM}_{\delta \mathrm{O_3}}$ the atmospheric parameter H_2O and O_3 has not be considered within the basis coordinate system, hence within the calculation of the basis LUT.

In our approach all parameters associated with an operator for that $\vec{I}_{\mathrm{Astate}}$ is an eigenvector are separated and not considered within the basis LUT and the respective operator processes are parameterised.

The remaining operators describe linear independent processes and the underlying atmospheric parameter is building the basis coordinate system.

2.3. Clear sky approach

2.3.1. The basis clear sky LUT

The basis clear sky LUT, containing the transmission for the linearly independent atmospheric clear sky radiation processes, consists of RTM results for aerosols with different Aerosol Optical Depth (AOD), single scattering albedo (ssa), and asymmetry parameter (gg). For the remaining parameters (water vapour, ozone, surface albedo), which correspond to linearly dependent processes, fixed values have been used for the calculation of the basis LUT: 15 kg/m^2 water vapour column, 345 DU ozone, and a surface albedo of 0.2. The effect of the solar zenith angle on the transmission, hence the solar irradiance, is considered by the use of the Modified Lambert Beer (MLB) function, leading to a huge reduction of the needed RTM calculations. The MLB function is discussed in detail in Mueller et al. (2004), including proof and verification of the MLB equations. In Section 2.3.2 only a short outline is given.

Using the basis LUT the atmospheric transmission can be derived for a given aerosol state by interpolation within the basis LUT for every SZA, but at this stage only for fixed water vapour, surface albedo and ozone values. In order to correct the effect of variations from the fixed values occurring in nature, the parameterisations described in Section 2.3.3, 2.3.4 and 2.3.5 are applied.

2.3.2. Sun zenith angle dependency — the modified Lambert–Beer function

The Lambert–Beer relation is given, within the scope of atmospheric application and monochromatic irradiance, by

$$B_\lambda = I_{0\lambda}{}^* \exp\left(\frac{-\tau_{0\lambda}}{\cos(\theta_z)}\right)^* \cos(\theta_z) \tag{2}$$

where $\tau_{0\lambda}$ is the optical depth of the vertical column, B_λ is the direct radiation (beam) at ground for a solar zenith angle (SZA) of θ_z and $I_{0\lambda}$ is the extraterrestrial irradiance at wavelength λ. Direct monochromatic irradiance derived with this formula agrees well with the SZA dependent diurnal variation of explicit RTM results. A good match for wavelength bands and solar surface irradiance and its diffuse fraction is only possible if an additional "empirical" correction exponent a is used. Hence a correction of the optical depth, or equivalent to this, of the parameter $\frac{\tau}{(\cos\theta_z)}$ is necessary.

$$I_{\mathrm{basis}} = I_{0,\mathrm{enh}}{}^* \exp\left(\frac{-\tau_0}{\cos^a(\theta_z)}\right)^* \cos(\theta_z). \tag{3}$$

The fitting parameter a is calculated based on a two RTM runs, one at $\theta_z = 0$ and the other at $\theta_z = 60°$, hence the correction parameters a_i can be calculated without the need for a numerical fit. $I_{0,\mathrm{enh}}$ is based on the extraterrestrial irradiance at the top of atmosphere and estimated using Eq. (4). In order to match MLB function with RTM results I_0 has to be enhanced for solar surface irradiance and diffuse irradiance at low visibilities (high optical depth, high aerosol load). A general equation has been found which is applied to I_0 to get $I_{0,\mathrm{enh}}$. Hence, $I_{0,\mathrm{enh}}$ is used instead of I_0 for all atmospheric states.

$$I_{0,\mathrm{enh}} = \left(1 + I_0 \cdot \frac{I_{\mathrm{diffuse}}}{I_{\mathrm{direct}} \cdot I}\right) \cdot I_0. \tag{4}$$

Here I_{diffuse} and I_{direct} are the diffuse and direct fraction of the solar surface irradiance I. Using the MLB function (Eq. (3)) only RTM calculations at 2 SZA have to be saved in the LUT compared to 7–9 for "pure technical" LUTs, without significant reduction of accuracy. Using the so-called Modified Lambert–Beer (MLB) function, the calculated direct irradiance as well as the solar surface irradiance can be reproduced very well (see Fig. 2). Extensive validation results can be found in Mueller et al. (2004) and Ineichen (2006). It is important to notice that the fitting parameter a has different values for direct irradiance and solar surface irradiance.

2.3.3. Treatment of water vapour and ozone variations

RTM runs for the clear-sky case have been performed, in order to derive the atmospheric transmissivity correction for water vapour and

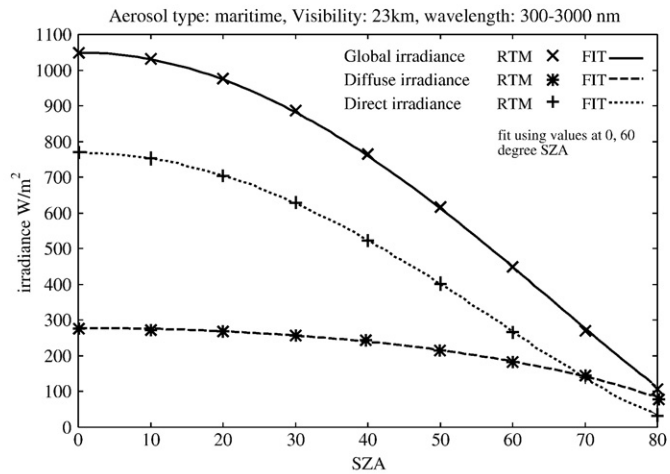

Fig. 2. Comparison between RTM calculations and fit using the modified Lambert–Beer relation. Example for a fit of broadband irradiance. Global irradiance is synonymous to solar irradiance at the surface. Direct irradiance is the direct portion (beam) of the solar surface irradiance.

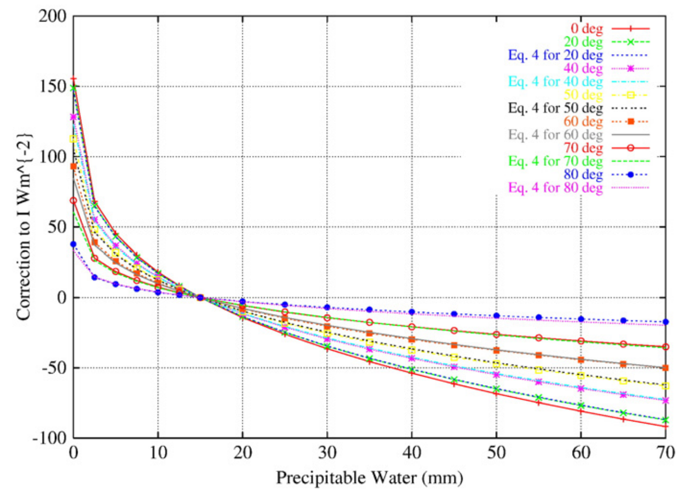

Fig. 3. Differences between I^{h2o}_{basis} and I_{basis} estimated by explicit RTM calculations and by use of the correction formula (Eq. (5)) for different solar zenith angles (0, 20, 40, 50, 60, 70, 80). The unit mm is equivalent to kg/m^2.

ozone variations relatively to the fixed standard values (15 kg/m^2 and 345 *DU*).

The effect of variations in water vapour and ozone is predominantly independent of the atmospheric state (e.g. the aerosol load) and the surface albedo. Consequently, a basis LUT is calculated with fixed water vapour and ozone amounts (15 mm, 345 DU). The effect of deviations of H_2O and O_3 on the solar irradiance relatively to the fixed values (used in the basis LUT) is quantified by application of the following correction:

$$I^{h2o}_{basis} = I_{basis} + \Delta I_{H_2O} \cdot \cos^a \theta_z. \tag{5}$$

I_{basis} is the solar irradiance at the surface *I* derived from the basis LUT for fixed water vapour amount of 15 mm, I^{h2o}_{basis} is the solar surface irradiance corrected for the actual water vapour amount, and θ_z is the solar zenith angle (SZA). ΔI_{H_2O} is the difference between *I* for the 15 kg/m^2 water vapour and the *I* for the actual amount of water vapour, for $\theta_z = 0$ and a fixed standard atmosphere defined by rural aerosol type with an AOD of 0.2, a surface albedo of 0.2 and 345 DU ozone. ΔI_{H_2O} depends on the amount of water vapour. It is pre-calculated for 18 water vapour amounts and the algorithm uses the appropriate ΔI_{H_2O} value for the specific pixel and time. Hence, for fixed solar zenith angle Eq. (5) is equivalent to Eq. (1) if we consider that I^{h2o}_{basis} is equal to $RTM_{\delta H2O}(\overrightarrow{I}_{Astate})$.

The validity of this formula was verified, and the best *a* value was found to be 0.88. The accuracy of this method is visualised in Fig. 3, which illustrates the quite small differences between explicit RTM runs and results derived using Eq. (5). The deviations are negligible (considerably below 1 W/m^2) for the majority of cases. Only for extreme conditions (high SZA, very high or low amount of water vapour), deviations between explicit RTM runs and parameterisation up to 5 W/m^2 can occur. However, small H_2O amounts (<2 kg/m^2) are unlikely to occur within the MSG disk and for H_2O amounts above 65 kg/m^2 the error and uncertainty of H_2O retrieval increases significantly due to saturation. Hence the parameterisation performs well (deviations below 1 W/m^2) for realistic atmospheric conditions and water vapour retrievals.

For ozone the same approach (form-invariant equation) is used. However the effect of ozone on the broadband solar surface irradiance is quite small, therefore only three pre-calculated ΔI_{O3} values are needed.

2.3.4. Correction of surface albedo

RTM calculations for a manifold of atmospheric states has been performed investigating the interaction of surface albedo and atmospheric clear sky state (aerosol load, water vapour, ...). The effect of the surface albedo on the solar surface irradiance is predominantly independent on the atmospheric clear sky state. This enables the linearisation and parameterisation of the surface albedo effect on the solar surface irradiance, leading to the following formula.

$$I = I^{h2o}_{basis} * (0.98 + 0.1 \cdot \mathrm{SAL}) \tag{6}$$

I^{h2o}_{basis} is the solar surface irradiance derived from the basis LUT for a surface albedo of 0.2 after Eq. (5) has been applied. SAL is the variable surface albedo and *I* is the solar irradiance after the surface albedo correction has been applied. Fig. 4 illustrates the predominantly linear behaviour of the surface albedo.

2.3.5. Sensitivity on atmospheric background profiles

The atmospheric background profile provides the vertical information on the total number density needed for the calculation of the Rayleigh scattering. In addition, it provides the vertical profile of water vapour and ozone, which are scaled according to the column amounts. Yet, using different background profiles (e.g. mid-latitude summer, polar winter, ...) has predominantly no effect on the solar surface irradiance. Consequently, in the new approach all RTM calculations are

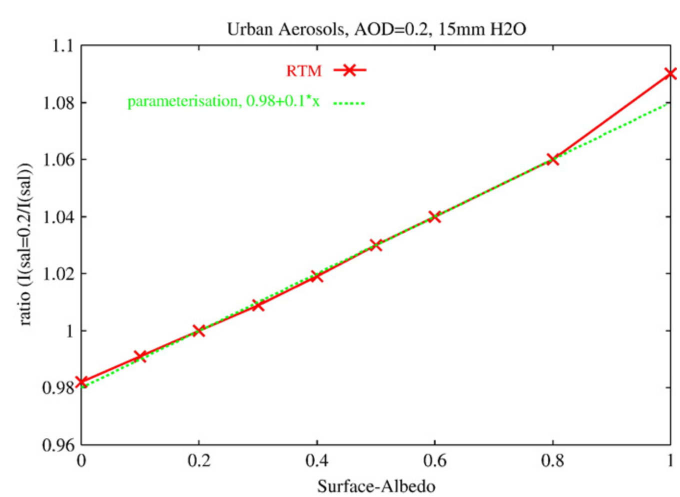

Fig. 4. The ratio between the solar surface irradiance *I* for a fixed surface albedo of 0.2 and *I* for variable surface albedos. The dotted line corresponds to Eq. (6), and the solid line to explicit RTM runs. The RTM behaviour agrees well with the parameterisation of Eq. (6) in its linear region.

Table 1
Reduction of needed RTM runs, comparison of original prototype CM-SAF algorithm, compared with the new algorithm.

Parameter	RTM runs Prototype	RTM runs New concept	Method
Background atmosphere	5	1	RIA
Aerosol AOD and type	*10 *8	*10*3*2	ssa and gg instead of 8 types
Solar zenith angle	*8	*2	MLB function
H_2O,O3	*10 *5	+18 +3	PCA as basis for parameterisations
Surface albedo	*8	+0	PCA as basis for parameterisation
Total number of RTM calculations	1,280,000	181	

RIA: RTM based impact analysis, PCA: Analysis of Principal Components and Symmetries based on RTM studies, MLB: modified Lambert–Beer relation.

only performed for the US standard atmosphere rather than for 5 atmospheric background profiles as before in the CM-SAF prototype.

2.3.6. Summary of clear sky approach

The basis look-up tables has been calculated for several aerosol optical depths and types and 2 sun zenith angles with fixed values of surface albedo (0.2) water vapour column (15 mm) and ozone (345 DU). The effect of variations in water vapour, ozone and surface albedo relative to the fixed values used in the calculation of the basis LUT is corrected by using the described correction formulas and parameterisation. Due to optimisations of the interpolation grid and the application of the water and ozone correction as well as the surface albedo parameterisation the amount of needed RTM calculations is enormously reduced. Applying the new method reduces the needed RTM calculations by a factor of 10,000 without loosing accuracy. Table 1 illustrates the reduction of the needed RTM calculations. Contrary to the previous CM-SAF prototype algorithm, the clear-sky model no longer relies on top of atmosphere flux densities.

Fig. 5 illustrates the new clear-sky scheme and the context and order of the parameterisations.

2.4. Cloudy sky approach

The Geostationary Earth Radiation Budget (GERB) instrument has been especially developed for the monitoring of the Earth radiation budget at the top of the atmosphere. GERB has been the motivation to develop a cloudy scheme that is able to use the top of atmosphere radiation derived from GERB as input. However, any other satellite instrument suitable for the retrieval of the top of atmosphere (TOA) albedo could also be used instead from a pure technical point of view. The need to relate the atmospheric transmittance to the top of atmosphere albedo to retrieve the surface irradiance in cloudy cases, introduces more complexity related to the clear sky case. Therefore some of the parameterisations described for the clear sky situations cannot be applied to cloudy situations, for example the parameterisation of the surface albedo effect. The parameterisation for the ozone and water vapour absorption has to be extended to the top of atmosphere albedo. However, the basic approach (Section 2.1 and 2.2), calculating a basis LUT using parameters involved in linear independent processes and parameterisation of the "eigenvector" processes is identical to the clear-sky case.

2.4.1. The basis cloudy sky LUT

For the calculation of the LUTs, additional parameters introduced by the presence of clouds have to be treated. This is performed by using a standard cloud parameterisation of Hu and Stamnes (1993) with varying cloud optical depth (COD) and effective droplet radius of 10 µm. 10 µm is an appropriate average radius of droplets in non-precipitating water clouds (Kokhanovsky, 2006) and has also been used by e.g. Bishop and Rossow (1991) and Lohmann et al. (2006) within the retrieval scheme of solar surface irradiance and by Bäuml et al. (2004) for the investigation of the PPH-bias on reflectivity and transmissivity. Bäuml et al. (2004) mentioned that setting the effective radius to a value of 10 does not change the results noticeably. Also Siegel et al. (1999) reported that reasonable variations in cloud droplet radius do have a minimal effect on the incident spectral flux densities (VIS wavelength region).

Implementation of a variable effective droplet radius would be straightforward as it would be not linked with the need of a huge amount of RTM calculations, a significant advantage of the method discussed in this paper. However, the positive effect of using a variable effective droplet radius from operational remote sensing has to be demonstrated beforehand. So far we found no negative effect on accuracy compared to the prototype, which uses variable effective droplet radii.

For homogeneous clouds (idealised RTM cloud) the relation between the top of atmosphere albedo and the transmission is predominantly linear for varying COD, independently of the atmospheric state (see Fig. 6). This has been found by 1D-RTM calculations for different atmospheric states and is consistent with the findings reported in literature, e.g. Li et al. (1993) and Pinker et al. (1995) and references therein. As a consequence, RTM results are only saved for a COD of 12 and 160, which is enough to describe the linear behaviour between transmission and top of atmosphere albedo of 1D-RTM in cloudy

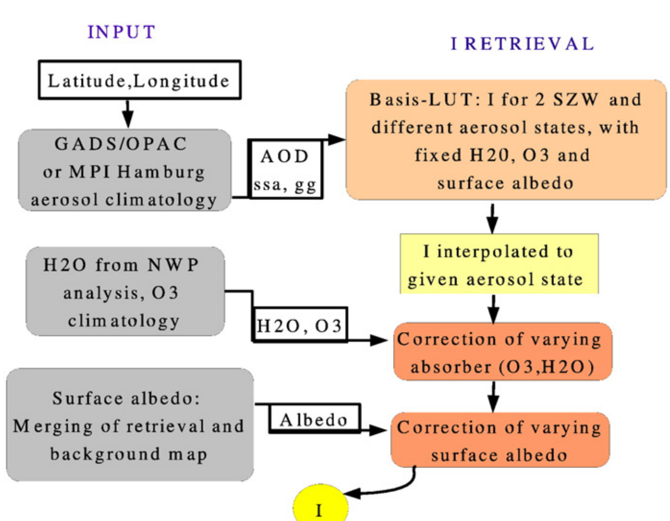

Fig. 5. Diagram of the new clear sky LUT. NWP stands for Numerical Weather Prediction. *I* is the solar surface irradiance.

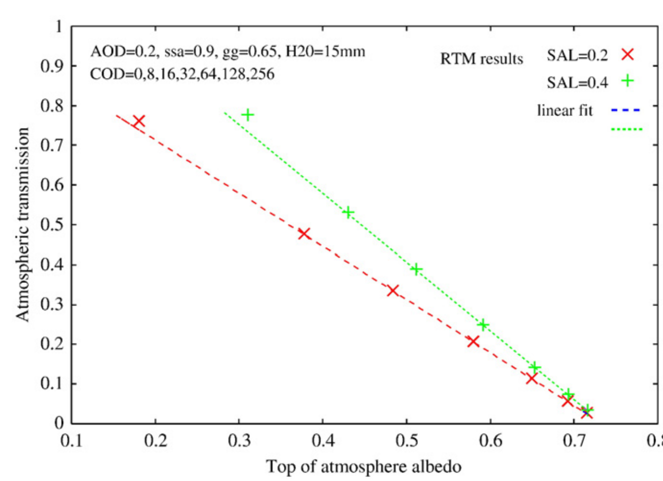

Fig. 6. The figure illustrates the linear behaviour between the transmittance and the top of atmosphere albedo for homogeneous (idealised RTM cloud) clouds. RTM results are diagrammed together with a linear fit. The linear fit matches well with exception of the RTM result for a COD of zero (clear sky).

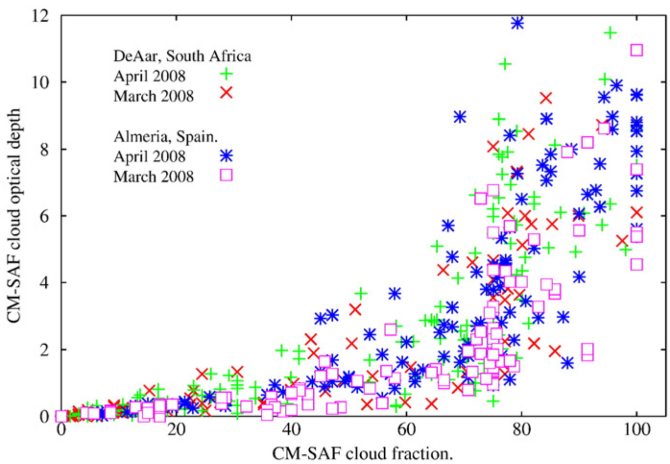

Fig. 7. Cloud fractional cover (CFC) and respective Cloud optical depth (COD) for Almeria, Spain and De Aar, Africa for March and April 2008. Both quantities are operationally retrieved from Meteosat-9 within the CM-SAF network. The COD and CFC retrieval algorithms are independent from the *I* retrieval method and described in detail in the respective Product User Manuals (PUMs). Both CM-SAF products as well as the PUMs are public available on www.cmsaf.eu.

situations. Only in the transition zone between clear-sky and homogeneous clouds (assuming fully cloudy pixel) with low CODs the behaviour is non-linear. However, in this region it cannot be assumed that the pixels are fully cloudy any more.

The cloud optical depth used as input for the RTM calculations is clearly related to the clearness index, which is defined as the surface solar irradiance divided by the extraterrestrial solar irradiance. The amount of beam irradiance calculated with a 1D-RTM assuming entirely cloudy pixels for COD ranging between 12 and 0 is in clear disagreement with empirical findings and validated semi-empirical methods for the estimation of beam and diffuse fraction respectively (Skartveit et al., 1998; Gonzalez & Calbo, 1999; Miguel et al., 2001; Ineichen et al., 2009). For example, the beam calculated with a 1d-RTM assuming entirely cloudy pixel is zero for SZA of 30 and COD of 10 but the beam fraction for the corresponding clearness index is around 15%. The disagreements can only be resolved by a significant frequency of partly cloudy pixels below a COD of 12 increasing with decreasing COD. Fig. 7 illustrates the relation between cloud optical depth and cloud fraction at two sites. Besides the large scattering of the data it is evident that the assumption of totally cloudy pixels is statistically incorrect for low COD values. As a consequence, the transmittance is interpolated between the clear-sky transmittance and the transmittance of a entirely cloudy pixel with a COD of 12. We assign a cloud coverage linearly increasing between 0 and 100% for COD between 0 and 12, the linear relation as well as the upper COD boundary might to be optimised empirically in the future. As a consequence of the arguments given above 3 COD values (0, 12, 160) have been evaluated to be sufficient, reducing the needed RTM runs significantly.

In contrast to the clear-sky case, the surface albedo cannot be parameterised or linearised due to its non-linear interaction with the top of atmosphere albedo in the presence of clouds. At least at this stage we have not found an accurate parameterisation. Therefore, the surface albedo is considered explicitly within the basis LUT.

The TOA albedo–transmissivity relationship is described by the basis LUT for different aerosol states, 3 cloud optical depths, and 8 surface albedos. The TOA albedo–Transmissivity relationship is used at each pixel to derive the transmissivity t and hence the solar irradiance I.

The water vapour and ozone values are fixed within the basis LUT and the effect of variations are considered similarly to the clear-sky case. The problem addressed here is how to adapt the correction of solar surface irradiance ΔI due to different water vapour and ozone, for various solar zenith angles θ_z and surface albedos SAL. The correction has to be applied both to the surface irradiance and for the outgoing TOA flux density, which introduces more complexity.

2.4.2. Treatment of water vapour and ozone variations

In the basis cloud look-up table the relation between the top of atmosphere albedo and the transmittance (hence the solar irradiance at the surface) is pre-calculated for a lot of different surface and aerosol states but for fixed values of water vapour and ozone. The effect of water vapour on the solar surface irradiance is, of course, different to that on the outgoing top of atmosphere flux density. The surface albedo significantly effects the water vapour and ozone correction equation (Eq. (5)) of the solar irradiance at the top of atmosphere, but not at the surface. Additionally the dependency on the cloud optical depth is different. This is the reason why the relation between the transmittance and TOA albedo is performed in a two step approach, applying the correction on the pre-calculated TOA albedo and transmittance separately, leading finally to a corrected relation between the top of atmosphere albedo and the transmittance. It is important to note that the correction described in Section 2.4.2.2 is applied to correct the relation between the transmittance and top of atmosphere albedo for the actual values of water vapour and ozone relative to the fixed values used in the basis LUT. During the operation of the scheme the corrected relation between transmission and top of atmosphere is used to find the associated transmission to the top of atmosphere albedo derived from satellite (e.g. GERB). This satellite based Top of Atmosphere Albedo is an input parameter and is not corrected or modified by Eq. (7). The correction Eq. (7) effects only the relation between the pre-calculated transmittance (hence I) and the top of atmosphere albedo (hence the outgoing flux density), which is saved in the basis LUT for fixed values of water vapour and ozone.

2.4.2.1. Correction of atmospheric transmittance. It has been evaluated by RTM calculations that the correction of water vapour deviations from the fixed values used for the calculation of the basis LUT follows a similar form to Eq. (5), applied for clear-sky situations. In cloudy situations the same equation can be used, but this time ΔI_{H_2O} and a are functions of the cloud optical depth τ. The dependence of a on τ is illustrated in Fig. 8. Exponent a does not depend on the surface albedo. ΔI_{H_2O} depends significantly on τ and the surface albedo and has therefore to be pre-calculated for every τ and surface albedo value of the interpolation grid.

The accuracy of applying Eq. (5) in the cloudy-sky case is shown in Fig. 9. The legend of this figure is the same as in Fig. 3. Similar to the case of clear-sky, the error introduced from the use of Eq. (5) is in the order of a few W/m^2.

Furthermore, a appears to be insensitive to the different aerosol loadings of the atmosphere. Several different atmospheric states have been investigated, with AOD, ssa and gg ranging from 0.1 to 0.45, 0.8 to

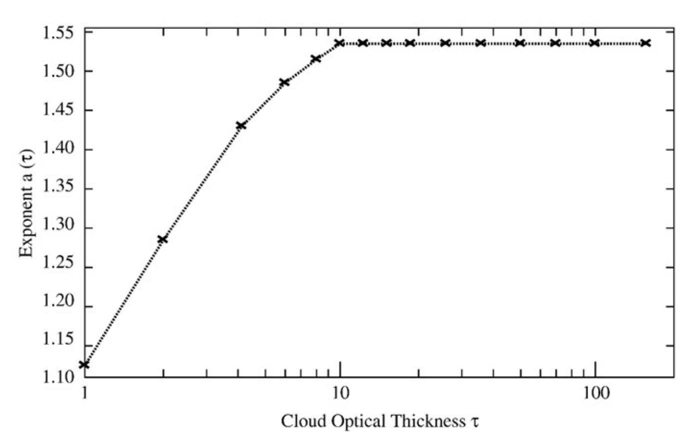

Fig. 8. Dependence of exponent a on the cloud optical thickness τ for the solar surface irradiance in cloudy situations.

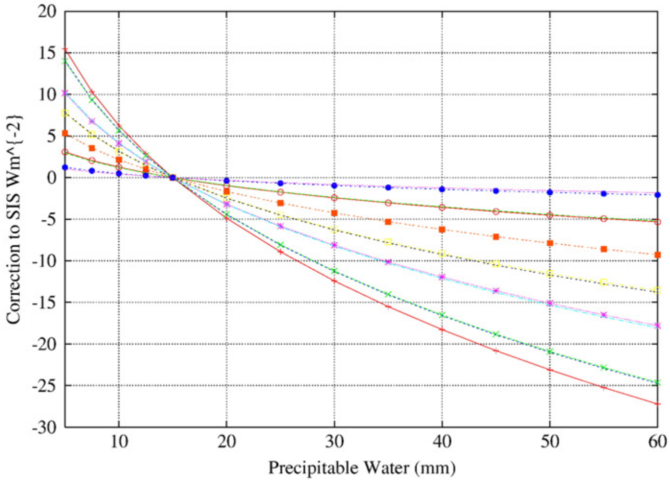

Fig. 9. Differences between $I_{\mathrm{basis}}^{\mathrm{h2o}}$ and I_{basis} estimated by explicit RTM calculations (dots) and by use of the correction formula (Eq. (5), lines) for different solar zenith angles (0, 20, 40, 50, 60, 70, 80) and a τ of 25.

0.96 and 0.67 to 0.77, respectively. ΔI_0 values were slightly different for each case, but a showed almost no sensitivity.

Five different combinations of low, middle, and high clouds were used as cloud configurations when running libRadtran. The effect of different cloud configurations (cloud height, cloud thickness) on a is negligible. The different cloud configurations created differences on ΔI_0 which were 1–2 W/m^2. These differences are small enough for the cloud configuration effect to be neglected.

2.4.2.2. Correction for top of atmosphere flux density. Again, we can use an equation of the form of Eq. (5)

$$I_{\mathrm{refl}} = I_{\mathrm{refl,basis}} + \Delta I_{\mathrm{refl,H_2O}} \cos^a \theta_z \tag{7}$$

to correct for the effect of water vapour variations on the top of atmosphere outgoing flux density, hence the top of atmosphere albedo.

$\Delta I_{\mathrm{refl,H_2O}}$ is the correction to I_{refl} due to water vapour deviations from the basis value of 15 kg/m^2 at a solar zenith angle θ_z of zero. Similar to $\Delta I_{\mathrm{H_2O}}$, the $\Delta I_{\mathrm{refl,H_2O}}$ and a vary very little with the aerosol state of the atmosphere. Exponent a depends on the cloud optical thickness τ, as in the case of the cloudy-sky surface irradiance. It should be noted that for τ values in the range 0–10, the fit of Eq. (7) is not very good, but this is not crucial as the transmittance for these partly cloudy region is interpolated. Furthermore, the errors in $\Delta I_{\mathrm{refl,H_2O}}$ are less than 5 W/m^2. The fit works quite well for CODs above 10. Fig. 10 shows an example of the fit accuracy for a COD of $\tau = 25$.

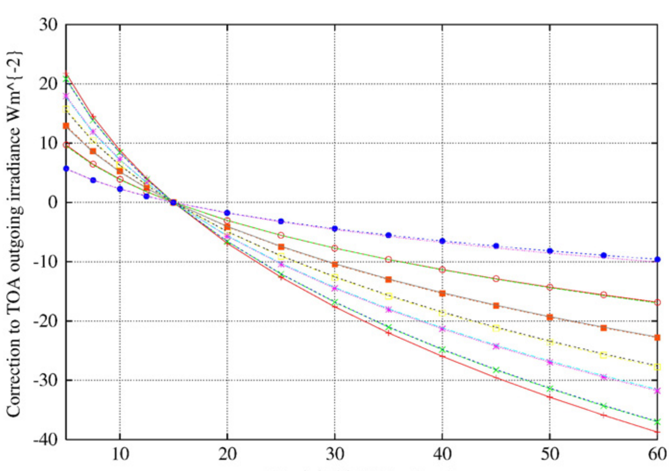

Fig. 10. Differences between I_{refl} and $I_{\mathrm{refl,basis}}$ estimated by explicit RTM calculations (dots) and by use of the correction formula (Eq. (7), lines) for different solar zenith angles (0, 20, 40, 50, 60, 70, 80) and a τ of 25.

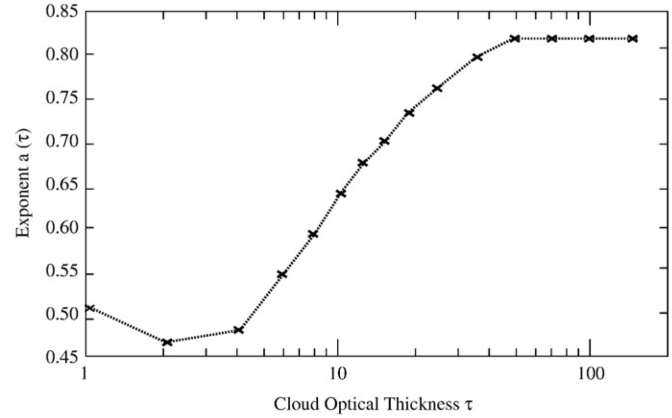

Fig. 11. Dependence of exponent a for the top of the atmosphere on the cloud optical thickness τ, for a surface albedo of 0.2.

For the outgoing TOA flux density, a depends also on the surface albedo. In Fig. 11 the dependence of a on τ for a surface albedo of 0.2, the value used within the calculation of the basis LUT, is shown. Five different combinations of low, middle, and high clouds were used as cloud configurations when running libRadtran. Exponent a practically does not vary with different cloud configuration files. However, $\Delta I_{\mathrm{refl,H_2O}}$ can be quite different between ice and water clouds. This effect has been neglected in this approach, but it could be implemented. However, this would increase the amount of necessary RTM calculations and has to be proven to increase the accuracy beforehand.

2.4.3. Summary cloud LUT approach

The basis look-up tables has been calculated for three cloud optical depths, 10 aerosol optical depths, 3 single scattering albedos and 2 asymmetry parameters, 6 sun zenith angles and 7 surface albedos. The effect of variations in water vapour and ozone relative to the fixed values used in the calculation of the basis LUT is corrected by using the described correction formulas (Eq. (5) and (7)). Due to optimisations of the interpolation grid and the application of the water and ozone correction the amount of needed RTM calculations is still small compared to the CM-SAF prototype LUT approach, in detail 10^3 instead

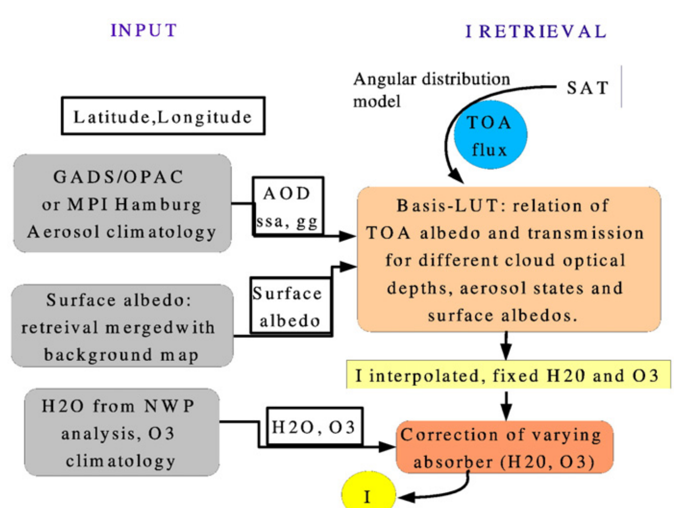

Fig. 12. Diagram of the new cloudy sky LUT.

of 10^7 Fig. 12 illustrates the new cloud scheme and the context and order of the parameterizations.

The cloudy sky LUT contains the clear sky case. Using the cloud LUT also for clear sky situations would be technically no problem, but would increase the uncertainty of the retrieved solar surface irradiance. The relation between transmission and top of atmosphere albedo relies strongly on the surface albedo, especially for clear sky. The CM-SAF surface albedo product (SAL) has an accuracy of 20% (relative deviation). As SAL has a significant smaller effect on the clear sky transmission than on the TOA albedo the cloudy sky LUT is currently not used to retrieve the solar surface irradiance for cloud free situations. This can be changed once the SAL accuracy is further improved.

3. Validation of the retrieved CM-SAF solar surface irradiance

3.1. Used input on the atmospheric state

The information on the cloud fraction is derived with the nowcasting SAF (SAFNWC) software (Derrien & LeGLeau, 2005), which is available at the SAFNWC web page (http://nwcsaf.inm.es/). The CM-SAF surface albedos are retrieved from the satellite information for each cloud free pixel using a algorithm developed by the Finish Meteorological Institute. Narrow-band surface reflectance is computed from the TOA reflectance by atmospheric correction (taking into account aerosols and absorbers) using the SMAC method (Rahman & Dedieu, 1994). Viewing and illumination conditions are corrected using the BRDF (Bidirectional Reflectance Distribution Function) correction (Li et al., 1996). Finally, a method presented by Liang (2000) is used for converting the narrowband albedo to broadband albedo. In cloudy cases, when the surface albedo cannot be retrieved, background values based on the USGS land-cover map (Brown et al., 1993) are used. A formula given in Dickinson (1983) is applied in order to consider the solar zenith angle dependency of SAL. Aerosol information is taken from the GADS/OPAC climatology (Hess et al., 1998) using NCEP (Kalnay et al., 1996) relative humidity in order to consider the effect of relative humidity on aerosol optical depth, single scattering albedo and asymmetry parameter. The water vapour profile results from the analysis of the global NWP model of the German Weather Service. The top of atmosphere albedo is generated by the Royal Meteorological Institute of Belgium (RMIB), based on GERB data (Harries et al., 2005).

3.2. In-situ data

It is quite important to use well-maintained ground based stations equipped with regularly calibrated instruments. Otherwise the validation results lead easily to misleading conclusions on the accuracy and precision of the validated product and are therefore worthless.

The radiation data used for the validation of the CM-SAF radiation products are mainly taken from BSRN (Baseline Surface Radiation Measurement) sites (Ohmura et al., 1998). The non-systematic errors for the BSRN data are estimated to be 10 W/m^2 for the long-wave measurements and 5 W/m^2 for solar surface irradiance measurements (Ohmura et al., 1998). Lindenberg, Carpentras and Payerne are BSRN stations. However, due to the gaps in the official BSRN archive the data of these stations have been directly received by the respective National Meteorological Services (NMS). The data from the Plataforma Solar de Almeria, have been accepted in the BSRN database in 2006 and has also been achieved directly.

Finally, data from the station Belsk (Institute of Meteorology and Water Management, Poland) and the ENTPE station of Lyon (http://idmp.entpe.fr/vaulx/stafr.htm), which is part of the IDMP (International Daylight Measurement Programme), has been used (Mardaljevic, 2001).

For the validation, CM-SAF data based on MSG are available from 2006 onwards. For specific validation studies in arid and semi-arid regions, with special focus on the African continent, CM-SAF products has been generated for July and October 2004.

The stations used for the validation are located in different sites in Europe and Africa covering different climates, ranging from continental, maritime to arid and semi-arid regions.

3.3. Validation results

3.3.1. "Operational" validation of monthly means

CM-SAF performs an ongoing regular validation and bias monitoring for 6 reference stations in Europe. The validation results are a good basis to define the accuracy and stability of the retrieved product for Europe.

The CM-SAF monthly means are calculated following a method by Möser and Raschke (1984), also published in Diekmann et al. (1988).

$$I_{\mathrm{dm}} = I_{\mathrm{clear,dm}} \cdot \frac{\sum I_i}{\sum I_i^{\mathrm{clear}}} \tag{8}$$

in order to take care of data gaps. Here I_{dm} is the daily mean, $I_{\mathrm{clear,dm}}$ the clear sky daily mean and I_i the calculated solar surface irradiance for satellite image i and I_i^{clear} the corresponding calculated clear sky value. The use of the formula improves also the accuracy of daily and monthly means from polar orbiting satellites, as they have a relative low temporal frequency outside the polar region.

The monthly mean of the pixel located above the respective measurement site is extracted and compared with the monthly mean of the ground measurement. Ground measurements are available in high temporal resolution (1 min, Lindenberg 10 min means) and are arithmetically averaged in order to derive the daily means, whereby I is set to zero if solar zenith angle is greater than 90°. Statistically meaningful daily means are ensured by the proof of the valid radiation values used to calculate the daily mean. The arithmetic average of the daily means leads to the monthly mean.

Extensive details about the validation procedure and results can be found in the official and reviewed CM-SAF validation reports, public available at the CM-SAF web-page (www.cmsaf.eu.de, Documentation). Here a summary of the validation results is given in order to provide clear and concise information about the accuracy of the retrieved surface solar irradiance product.

Table 2 gives an overview of the validation results, including information on the ground based stations used. A target accuracy of 10 W/m^2 for monthly means has been defined within the scope of CM-SAF project. The selection of the target accuracy was based on expected accuracies needed for climate analysis and monitoring in the synoptic scale (WCRP, 1986 (Suttles & Ohring, 1986)). The accuracy of the CM-SAF products is close to the confidence level of the ground based measurements and significant better as the target accuracy, demonstrating the high accuracy of the CM-SAF irradiance.

The monthly bias values are below 10 W/m^2 for almost all months and stations. Only in March 2006 higher bias values occur in

Table 2
Results of the operational validation and bias monitoring of the CM-SAF solar surface irradiance in Europe, together with brief information on the stations used.

Station	Latitude°	Longitude°	Height in m	Number months	GBM W/m^2	MAB W/m^2	MBD W/m^2	RMSD W/m^2
Payerne	46.81N	6.94E	491	16	129.7	5.9	−3.9	6.6
Carpentras	44.05N	5.03E	100	12	146	3.7	3	4
Lindenberg	52.22N	14.12E	125	16	115.5	4.0	−3.9	3.7
Cabauw	51.97N	4.93E	2	15	114.7	3.9	0.5	4.5
Belsk	51.7N	20.8E	180	16	122.3	6.7	−6.7	6.5
Lyon	45.78N	4.93E	197	19	128	5.6	5.0	6.9

All results are based on comparison of monthly means. MAB=mean absolute bias (synonymous to mean absolute error), MBD=mean bias deviation, RMSD=root mean square deviation, GBM=mean of ground based measurement, n=number. The correlation coefficient is close to 1 for all stations and therefore not given in the table.

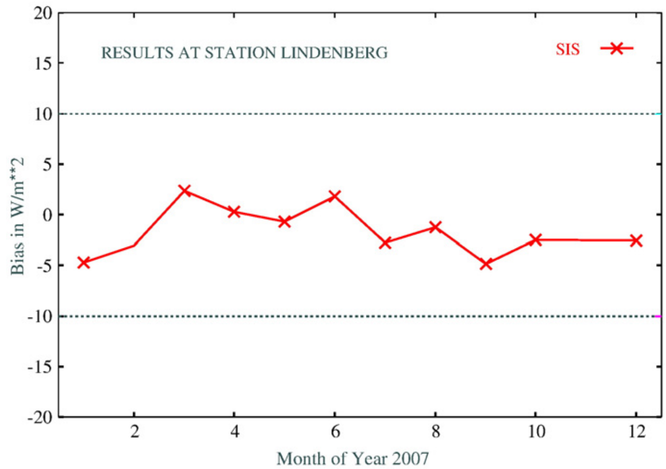

Fig. 13. Bias in W/m^2 between CM-SAF solar surface irradiance and ground measurement at the station Lindenberg for 2007.

Lindenberg and Payerne due to abrupt and extreme snow fall and snow cover. With the exception of the extreme snow event the bias shows no specific seasonal pattern nor a trend, indicating the seasonal stability of the CM-SAF product.

The CM-SAF users will be regularly informed about the status of the accuracy of CM-SAF products within annual validation reports, public available at the CM-SAF web-page (www.cmsaf.eu). Fig. 13 is extracted from the recent CM-SAF annual validation report. It shows the bias of monthly mean CM-SAF solar surface irradiance compared to the ground measurement at the station Lindenberg, together with the target accuracy of 10 W/m^2 as straight lines.

3.3.2. Validation for arid and semi-arid regions focusing on the African continent

Unfortunately, for the African stations the overlapping time period where both ground measurements and CM-SAF solar surface irradiance are available covers only 2 months. The African sites are not part of the operational validation of monthly means as a consequence, but investigated within a specific validation study. For these reason the validation over the African continent as well as the validation for the semi-arid region of Southern Spain is based on the comparison of instantaneous values. Comparison of instantaneous values means that the solar surface irradiance retrieved at the specific scanning time T_{scan} of the pixel located above the measurement site is compared to the respective ground measurement. The ground measurements used for the comparison are available in a 1 min resolution, hence the ground measurement at time T_{scan} is compared with the satellite based value at the same time T_{scan} within the "time uncertainty" of 1 min. The ground based measurement is a point measurement, while the satellite provides and pixel area average, which increases the RMSD.

Table 3 provides information about the stations used for the validation.

The solar surface irradiance is characterised by very high variations and values of zero in the night. Consequently, the error quantities of the monthly means and the monthly error quantities of the instantaneous values are not identical. In order to get a meaningful evaluation of the expected accuracy for the monthly mean climate product the bias in per cent is the more relevant quantity in the interpretation of the *I* validation results. With respect to the absolute bias in W/m^2 it has to be considered that the bias for the monthly mean can be expected to be about 50% lower. Of course the "real value" depends on the amount of night hours.

Table 3
List of in-situ stations used for the validations in arid and semi-arid climate.

Station	Latitude	Longitude	Country	Elevation (m)	Network
Tamanrasset	22.78°N	5.52°E	Algeria	1300	BSRN
Sede Boger	30.87°N	34.77°E	Israel	500	BSRN
De Aar	30.68°S	24.00°E	South Africa	1287	BSRN
Almeria	37.08°N	2.35°W	Spain	505	BSRN

Table 4 presents the overall validation results. The mean bias deviation over all stations and months for the instantaneous values is 2 W/m^2 and 1.3%, the respective mean RMSD is 20.62 W/m^2. However, for climate applications the mean absolute bias (the mean absolute error) is more relevant as error quantity. The mean absolute bias of the instantaneous values is with 13.2 W/m^2 and 3.1% quite small. The African stations alone (without Almeria) have a MAB of 14.4 and 2.8% respectively.

The GADS/OPAC aerosol climatology used as input for the *I* calculation is based on a quite rare data basis in Africa (Koepke, personal communication), hence the errors introduced by the aerosol climatology are not well known, but the validation results indicate that the used aerosol climatology provides reasonable monthly values for Africa. Taking into account the uncertainties and the non-systematic errors of the in-situ measurements the validation results clearly indicate that high accuracy can be also expected in arid and semi-arid regions of Africa.

3.3.3. Comparison over sea

In order to monitor the accuracy of satellite based radiation data, validation with well maintained and calibrated ground based measurements is necessary. Over sea, however, accurate reference data from calibrated instruments measuring radiation are scarce. There exist buoy measurements and also a measurement platform in the North sea (FINO), but the focus of their measurement activities is not radiation and their data are not well suited for validation studies, due to salt pollution of the instruments. Data from the German research vessel Meteor are used to fill this gap and to perform reasonable validation over sea. The track of the vessel is illustrated in Fig. 14.

To compare the ship based data, a daily average of all 10-minute measurements during the daily cruise have been averaged and assigned to the midday position of the Meteor vessel. These daily means have then been compared to the daily mean extracted from satellite. This kind of comparison introduces differences which are not due to errors in the satellite retrieval but due to the movement of the ship. In order to minimise this effect the results presented in Table 5, are therefore restricted to the cases where RV Meteor remained within a 15 km radius relative to the 12 UTC position (roughly 50% of all days). The results, given in Table 5, complete the picture of CM-SAF solar surface irradiance characterised by a high accuracy in different atmospheric and surface characteristics. In this manuscript only a

Table 4
Comparison of instantaneous satellite derived and in-situ solar surface irradiance.

Location	Year	Month	Sat W/m^2	In situ W/m^2	Bias W/m^2	Bias %	RMSD %	COR
De Aar	2004	07	386.8	387.1	−0.3	−0.1	16.9	0.95
		10	537.9	523.5	14.4	2.7	21.5	0.94
Sde Boqer	2004	07	619.5	605.5	−13.9	2.2	10.1	0.99
		10	445.1	428.3	−16.8	−3.9	24.3	0.92
Tamanrasset	2004	07	554.9	564.7	−9.8	−1.7	23.0	0.94
		10	482.8	514.1	−31.3	−6.1	11.1	0.99
Almeria	2006	06	508.9	513.0	4.1	0.8	20.5	0.95
		07	571.0	559.6	11.4	2.0	19.4	0.94
		08	531.9	530.9	−1.1	−0.2	16.5	0.96
		09	447.5	463.1	15.6	3.4	26.2	0.91
		10	316.7	332.5	15.8	4.8	28.2	0.92
		11	272.7	288.5	15.7	5.5	24.3	0.93
		12	279.3	300.8	21.5	7.2	27.0	0.87

COR=correlation, sat= satellite based solar surface irradiance, in situ=ground based measurement. See Table 2 for the other shortcuts.

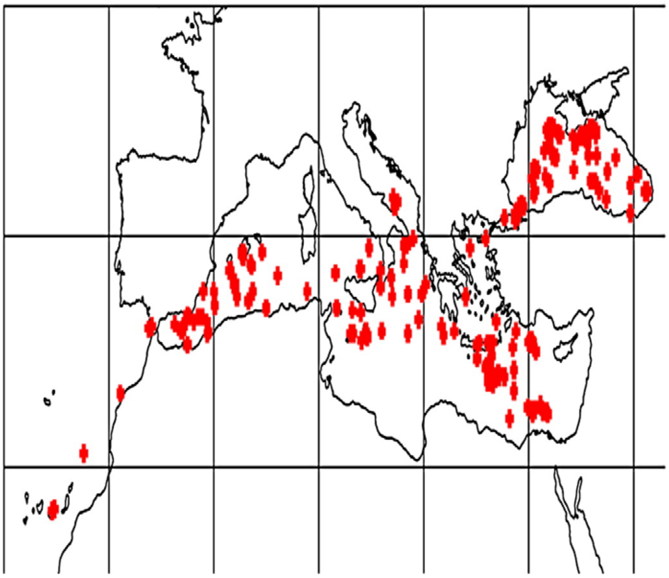

Fig. 14. Measurement sites of the vessel Meteor within the Mediterranean sea.

concise summary of the ocean validation is given. The validation procedure and results for the complete data set over sea are discussed and presented in detail in Behr et al. (in press).

4. Direct irradiance

The developed concept has also been applied to the retrieval of direct irradiance. In the clear sky case, the solar surface irradiance is estimated using the modified Lambert–Beer relation (Mueller et al., 2004). The same relation can be used for the calculation of the direct (beam) irradiance B, with the exception that instead of using $I_{0,\mathrm{enh}}$ the extraterrestrial irradiance I_0 can be used. Thus, the MLB relation is

$$B = I_0 \exp\left(\frac{-\tau_0}{\cos^a \theta_z}\right) \cos\theta_z \tag{9}$$

where θ_z is the solar zenith angle, τ_0 is the vertical optical depth, I_0 is the extraterrestrial irradiance, B is the direct irradiance at the surface, and a is a fitting parameter.

Analogously to the retrieval of the solar surface irradiance a LUT for τ_0 and a was calculated, for fixed water vapour and ozone amounts. The LUT is three-dimensional, with the dimensions corresponding to aerosol optical depth (10 values), single scattering albedo (3 values), and asymmetry parameter (2 values).

The atmospheric transmissivity correction due to water is following a similar equation to Eq. (5)

$$B^{\mathrm{H_2O}}_{\mathrm{basis}} = B_{\mathrm{basis}} \Delta B_{H_2O} \cos^a \theta_z \tag{10}$$

where B_{basis} is the direct irradiance from the LUT, $\Delta B_{\mathrm{H_2O}}$ is the correction due to water vapor variations for a zenith angle of 0 degrees, and $B^{\mathrm{H_2O}}_{\mathrm{basis}}$ is the water vapor-corrected direct irradiance for the zenith angle θ_z. The best a value was found to be 1.0. A similar formula is valid, when the correction with respect to ozone is considered.

$$B = B^{\mathrm{H_2O}}_{\mathrm{basis}} \Delta B_{\mathrm{O_3}} \cos^a \theta_z \tag{11}$$

where B is the water and ozone-corrected value and $\Delta B_{\mathrm{O_3}}$ is the correction only due to ozone for a zenith angle of 0°. In this case, the best a value is 0.7.

The $\Delta B_{\mathrm{H_2O}}$ and $\Delta B_{\mathrm{O_3}}$ values were pre-calculated and used directly from the algorithm during processing.

$\Delta B_{\mathrm{H_2O}}$ for the current water vapor and $\Delta B_{\mathrm{O_3}}$ for the current ozone values are found by interpolation and then Eqs. (10) and (11) are applied separately.

By this way the direct irradiance B is derived for clear-sky conditions. The extension to the cloud-contaminated or cloudy conditions (all-sky) is performed using the following relation between the cloudy sky direct radiation B_{all} and B:

$$B_{\mathrm{all}} = B[k - 0.38(1-k)]^{2.5} \tag{12}$$

where k is the clear-sky index. This formula is an adaptation of the Skartveit diffuse model (Skartveit et al., 1998).

Preliminary validation has been performed, indicating that the accuracy is better than 15 W/m^2, which is a very promising result. However, extended validation activities are needed and will be performed before final conclusions on the accuracy can be drawn. The results will be documented in a forthcoming paper.

5. Summary and conclusion

The paper describes the solar surface irradiance retrieval method used in the current operational CM-SAF processing scheme. The new method is based on radiative transfer modelling and enables the use of improved information on the atmospheric state within an operational processing. The extensive analysis of the interaction between the atmosphere, top of atmosphere albedo, surface albedo and solar surface irradiance has been the basis for a new concept, the combination of parameterisations and "eigenvector" look-up tables. The method implements several of the requirements discussed in Pinker et al. (1995) for the improvement of solar surface irradiance retrieval, e.g. the use of instruments with on-board calibration (top of atmosphere albedo from GERB) and the use of a cloud mask from improved cloud screening method (now-casting SAF cloud mask).

The MLB function (Mueller et al., 2004) is the first time applied within an "eigenvector" hybrid LUT approach. More over, a new concept for the adaptation of Skartveit–Olseth diffuse model within a physical scheme for the retrieval of direct irradiance is presented and discussed.

The results of the validation demonstrate the high accuracy of the model system. The mean absolute difference between monthly means of ground measurements and satellite based solar surface irradiance is 5 W/m^2 with a mean bias deviation of −1 W/m^2 and a RMSD of 5.4 W/m^2 for the investigated European sites. The results for the investigated African sites comparing instantaneous values are also encouraging. The mean absolute difference is with 2.8% even lower as for the European sites, being 3.9%, but the mean bias deviation is with −1.1% slightly higher as for the European sites, being 0.8%. The validation results over ocean in the Mediterranean Sea using ship borne data complete the validation, The mean bias deviation is −3.6 W/m^2 and 2.3% respectively. The slightly higher mean bias deviation over ocean is at least partly resulting from inherent differences due to the movement of the ship (shadowing, allocation of satellite pixel).

Without further optimisation, concerning the atmospheric input data and 3-d cloud biases, the accuracy is comparable to e.g. that of the well established Heliosat method (Drews et al., 2008, in press) as well as the OSI-SAF solar surface irradiance (Ineichen et al., 2009). The mean bias deviation of the CM-SAF solar surface irradiance (I) monthly means is with −1 W/m^2 slightly lower as that reported in a recently published method of Deneke and Feijt (2008) using CM-SAF

Table 5
Result for the ocean validation.

Station	Months	Satellite mean	Meteor mean	Bias	RMSD
Meteor vessel	Sep 2006–Jun 2007	160.7	157.1	−3.6	5.1

cloud products as input. The validation results also clearly indicate that the accuracy has been significantly improved relative to the prototype (Hollmann et al., 2006). The accuracy quantities also indicate that CM-SAF solar surface irradiance has a slightly better accuracy than surface solar irradiance from the International Satellite Cloud Climatology Project (ISCCP) (Bishop et al., 1997) and the solar surface irradiance derived from ISCCP data and the algorithms developed by the LaRC SRB group, Gupta et al. (1999) and references therein. However, the respective data has a lower spatial resolution than that of CM-SAF, which limits the comparability of the validation results. More over, Ineichen et al. demonstrated that the dispersion of Bias and RMSD at different measurement sites of the same method could be likely higher as the dispersion between different methods at identical sites and time periods (Ineichen et al., 2009). One reason for this finding might be due to the fact that the accuracy of surface solar irradiance depends significantly on the used and available input information of the atmospheric and surface state (Zhang et al., 2007). Finally, also ground measurements have their own specific errors and uncertainties. e.g. as regularly discussed at the BSRN meetings. As a consequence of the things mentioned above comparison of model performance based on accuracies given in publications is problematic and linked with the risk of over-hasty and misleading accuracy rankings and should be interpreted quite carefully. On the other hand this does also demonstrate the importance of direct inter-comparison of methods at identical sites and time periods for as many sites, time periods and climate regions as possible.

The CM-SAF retrieval for solar surface irradiance is able to outperform the CM-SAF target accuracy of 10 W/m^2 for monthly means. Indeed, the observed accuracies of the monthly means, expressed by the mean absolute bias, are close to the BSRN confidence level for the ground based measurements. The accuracy is significantly better than the 20 W/m^2 given in Pinker et al. (1995) as a benchmark for the validation of climate models. Consequently, the described retrieval scheme is well suited for climate monitoring and analysis applications e.g. Babst et al. (2008) and solar energy applications (Drews et al., 2008). However, in the quite heterogenous Alpine region higher uncertainties and higher errors than 10 W/m^2 occur due to missing dynamical snow cover information in high spatial resolution (Dürr et al., in press), which is predominantly not a drawback of the CM-SAF retrieval algorithm but of the used SAL input information.

The CM-SAF method for the retrieval of solar surface irradiance is characterised by a high computing performance going together with a high accuracy. In these terms, the method has also the potential to improve the treatment of radiation processes in climate models as well as in numerical prediction models. However, the model system can be improved by a semi-empirical adjustment of systematic heterogenous cloud effects as discussed e.g. in Girodo et al. (2006), Zinner and Mayer (2006) and Wyser et al. (2005) as well as by improved information on the atmospheric clear-sky state, especially concerning aerosols and snow cover maps in high spatial resolution (Dürr et al., in press). The developed method also includes the retrieval of direct irradiance. The first validation results of satellite based direct irradiance are encouraging.

Acknowledgements

Acknowledgement to D. Dumortier and ENTPE for the open, easy and free web-access to their high quality measurement data. Thanks to MeteoFrance, KNMI (The Royal Netherlands Meteorological Institute), MeteoSwiss, the plataforma solar de Almeria and the Institute of Meteorology and Water Management (Poland) for providing their high-quality in-situ data. This work is partially funded by the Eumetsat within the SAF framework. For providing the libRadtran RTM package we thank: Arve Kylling (NILU) and Bernhard Meyer (DLR). Thanks to the BSRN for the ground based data and to Flurin Babst for the correction of the English. We thank the NWC-SAF consortium for providing the NOAA/PPS and MSG/SEVIRI retrieval packages.

The authors are indebted to the work of the CM-SAF team in particular C. Koziar, D. Stein, S. Villbrandt, and R. Weber for supporting the technical development of the CM-SAF processing scheme, R. Cremer for supporting the validation activities, B. Thiess and P. Willing for handling the CM-SAF User Help Desk and finally W. Mehley for administrative support of the whole activity.

References

Babst, F., Mueller, R., & Hollmann, R. (2008). Verification of NCEP reanalysis shortwave radiation with mesoscale remote sensing data. *Geosciences and Remote Sensing Letters*, *5*(1).

Behr, H., Hollmann, R., Müller, R., in press. Surface radiation at sea: Validation of satellite-derived data with shipboard measurements. Meteorologische Zeitschrift.

Bishop, J., Rossow, W., & Dutton, E. (1997). Surface solar irradiance from the International Satellite Cloud Climatology Project 1983–1991. *Journal of Geophysical Resaerch*, *102*, 6883−6910.

Bishop, J. K. B., & Rossow, W. B. (1991). Spatial and temporal variability of global surface solar irradiance. *Journal of Geophysical Research*, *96*, 839−858.

Brown, J. F., Loveland, T., Merchant, J. W., Reed, B. C., & Ohlen, D. O. (1993). Using multi-source data in global land-cover characterization: concepts, requirements, and methods. *Photogrammetric Engineering and Remote Sensing*, *59*, 977−987.

Bäuml, G., Chlond, A., & Roeckner, E. (2004). Estimating the PPH-bias for simulations of convective and stratiform clouds. *Atmospheric Research*, *72*, 317−328.

Cano, D., Monget, J., Albuisson, M., Guillard, H., Regas, N., & Wald, L. (1986). A method for the determination of the global solar radiation from meteorological satellite data. *Solar Energy*, *37*, 31−39.

Darnell, W., Staylor, W., Gupta, S., Ritchey, N., & Wilber, A. (1992). Seasonal variation of surface radiation budget derived from ISCCP-C1 data. *Journal of Geophysical Research*, *97*.

Deneke, H., & Feijt, A. (2008). Estimation surface solar irradiance from METEOSAT SEVIRI-derived cloud properties. *Remote Sensing of Environment*, *112*, 3131−3141.

Derrien, M., & LeGLeau, H. (2005). MSG/SEVIRI cloud mask and type from SAFNWC. *International Journal of Remote Sensing*, *26*.

Dickinson, R. E. (1983). Land surface processes and climate — Surface albedos and energy balance. *Advances in Geophysics*, *25*, 305−353.

Diekmann, F. J., Happ, S., Rieland, M., Benesch, W., Czeplak, G., & Kasten, F. (1988). An operational estimate of global solar irradiance at ground level from METEOSAT data: Results from 1985 to 1987. *Meteorologische Rundschau*, *41*, 65−79 41.

Drews, A., Beyer, H., & Rindelhardt, U. (2008). Quality of performance assessment of PV plants based on irradiance maps. *Solar Energy*, *82*, 1067−1075.

Drews, A., Lorenz, E., Hammer, A., Heinemann, D., in press. Long-term accuracy assessment of satelite-derived global irradiance time series with respect to solar energy applications. Theoretical and Applied Climatology.

Dürr, B., Zelenka, A., Müller, R., Philipona, R., in press. Verification of CM-SAF and MeteoSwiss satellite based retrievals of surface shortwave irradiance over the Alpine region. International Journal of Remote Sensing.

Fontoynont, M., Dumortier, D., Heinemann, D., Hammer, A., Olseth, J., Skartveit, A., et al. (1997). Satellight: An European programme dedicated to serving daylight data computed from meteosat images. *Proceedings Lux Europa 1997. Vol. The 8th European Lighting Conference, Amsterdam* Http://www.satellight.com/indexgT.htm

GCOS (2003). *The second report on the adequacy of the global observing systems for climate in support of the UNFCCC. Vol. Rep. GCOS-82.* : WMO.

Girodo, M., Mueller, R., & Heinemann, D. (2006). Influence of three-dimensional cloud effects on satellite derived solar irradiance estimation — First approaches to improve the Heliosat method. *Solar Energy*, *80*.

Gonzalez, J. A., & Calbo, J. (1999). Influence of the global radiation variability on the hourly diffuse fraction correlations. *Solar Energy*, *65*, 119−131.

Gupta, S., Kratz, D., Stackhouse, P., & Wilber, A. (2001). *The Langley Parameterized Shortwave Algorithm (LPSA) for surface radiation budget studies. NASA/TP-2001-211272.*

Gupta, S., Ritchey, N., Wilber, A., & Whitlock, C. (1999). A climatology of surface radiation budget derived from satellite data. *Journal of Climate*, *12*, 2691−2709.

Hammer, A., Heinemann, D., Hoyer, C., Lorenz, E., Müller, R., & Beyer, H. (2003). Solar energy assessment using remote sensing technologies. *Remote Sensing of the Environment*, *86*, 423−432.

Harries, J., Russel, J., Hanafin, J., Brindley, H., Futyan, J., Rufus, J., et al. (2005). The Geostationary Earth Radiation Budget Project. *BAMS*, *86*.

Hess, M., Koepke, P., & Schult, I. (1998). Optical properties of aerosols and clouds: The software package OPAC. *Bulletin of the American Meteorological Society*, *79*, 831−844.

Hollmann, R., & Gratzki, A. (2003). *Scientific prototype report, surface incoming shortwave radiation. Tech. Rep. SAF/CM/DWD/PR/1.2A2,3, DWD,GKSS.* available at www.cmsaf.eu, Documentation.

Hollmann, R., Müller, R. W., & Gratzki, A. (2006). CM-SAF surface radiation budget: First results with AVHRR data. *Advances in Space Research*, *37*, 2166−2171.

Hu, Y., & Stamnes, K. (1993). An accurate parameterization of the radiative properties of water clouds suitable for use in climate models. *Journal of Climate*, *6*, 728−742.

Ineichen, P. (2006). Comparison of eight clear sky broadband models against 16 independent data banks. *Solar Energy*, *80*, 468−478.

Ineichen, P., Barroso, C., Geiger, B., Hollmann, R., Mueller, R., 2009. Satellite Application Facilities irradiance products: hourly time step comparison and validation. International Journal of Remote Sensing In press.

Kalnay, E., Kanamitsu, M., Kistler, R., Collins, W., Deaven, D., Gandin, L., et al. (1996). The NCEP/NCAR 40-year reanalysis project. *Bulletin of the American Meteorological Society*, *77*(3), 437−471.

Koepke, P., Bais, A., Balis, D., Buchwitz, M., de Backer, H., de Cabo, X., et al. (1998). Comparison of models used for UV index calculations. *Photochemistry and Photobiology*, *67*, 657−662.

Kokhanovsky, A. A. (2006). *Cloud Optics. No. ISBN-10 1-4020-3955-7 in atmospheric and oceanographic sciences library.* : Springer.

Li, Z., Cihlar, J., Zheng, X., Moreau, L., & Ly, H. (1996). The bidirectional effects of AVHRR measurements over boreal regions. *IEEE Transactions on Geoscience and Remote Sensing*, *34*(6).

Li, Z., Leighton, H., Masuda, K., & Takashima, T. (1993). Estimation of SW flux absorbed at the surface from TOA Reflected Flux. *Journal of Climate*, *6*(3).

Liang, S. (2000). Narrowband to broadband conversions of land surface albedo: I Algorithms. *Remote Sensing of Environment*, *76*.

Lohmann, S., Schillings, C., Mayer, B., & Meyer, R. (2006). Long-term variability of solar direct and global radiation derived from ISCCP data and comparison with reanalysis data. *Solar Energy*, *80*, 1390−1401.

Mardaljevic, J. (2001). The BRE-IDMP dataset: A new benchmark for the validation of illuminance prediction techniques. *Lighting Research and Technology*, *33*, 117−136.

Mayer, B., & Kylling, A. (2005). Technical note: The libradtran software package for radiative transfer calculations — Description and examples of use. *Atmospheric Chemestry and Physics*, 5.

Mayer, B., Seckmeyer, G., & Kylling, A. (1997). Systematic long-term comparison of spectral UV measurements and UVSPEC modeling results. *Journal of Geophysical Research*, *102*, 8755−8767.

Meyer, R., Hoyer, C., Schillings, C., Trieb, F., Diedrich, E., & Schroedter, M. (2003). SOLEMI: A New satellite-based service for high-resolution and precision solar radiation data for Europe, Africa and Asia. *ISES Solar World Congress 2003* http://elib.dlr.de/10027

Miguel, A., Bilbao, J., Aguiar, R., Kambezidis, H., & Negro, E. (2001). Diffuse solar irradiation model evaluation in the North Mediterranean Belt area. *Solar Energy*, *70*, 143−153.

Möser, W., & Raschke, E. (1984). Incident solar radiation over Europe Estimated from METEOSAT data. *Journal of Climate and Applied Meteorology*, *23*, 166−170.

Mueller, R., Dagestad, K., Ineichen, P., Schroedter-Homscheidt, M., Cros, S., Dumortier, D., et al. (2004). Rethinking satellite based solar irradiance modelling. the SOLIS clear-sky module. *Remote Sensing of the Environment*, *91*, 160−174.

Ohmura, A., Dutton, E., Forgan, B., Fröhlich, C., Hegner, H., Heimo, A., et al. (1998). Baseline Surface Radiation Network (BSRN/WCRP): New precision radiometry for climate research. *Bulletin of the American Meteorological Society*, *79*(10), 2115−2136.

Perez, R., Aguiar, R., Collares-Pereira, M., Dumortier, D., Estrada-Cajigal, V., Gueymard, C., et al. (2001). Solar resource assessment: A review. *Solar energy — The state of the art. No. ISBN 1 902916239 in ISES Position Papers* (pp. 497−562). London: James & James Science Publishers.

Perez, R., Renne, D., Seals, R., & Zelenka, A. (1998). The strength of satellite-based solar resource assessment. *Production of site/time-specific irradiances from satellite and ground data, report 98-3. New York State Energy Research and Development Authority, Corporate Plaza West, 286 Washington Avenue Extension, Albany, NY 12203-6399*.

Perez, R., Seals, R., & Zelenka, A. (1998). Production of site/time-specific hourly irradiances — Satellite remote sensing vs. network interpolation. *Production of site/time-specific irradiances from satellite and ground data, report 98-3. New York State Energy Research and Development Authority, Corporate Plaza West, 286 Washington Avenue Extension, Albany, NY 12203-6399*.

Pinker, R., & Laszlo, I. (1992). Modelling surface solar irradiance for satellite applications on a global scale. *Journal of Applied Meteorology*, *31*, 166−170.

Pinker, R. T., Frouin, R., & Li, Z. (1995). A review of satellite methods to derive surface shortwave irradiance. *Remote Sensing of Environment*, *51*, 108−124.

Rahman, H., & Dedieu, G. (1994). SMAC: A simplified method for the atmospheric correction of satellite measurements in the solar spectrum. *International Journal of Remote Sensing*, 15.

Rigolier, M., Levefre, M., & Wald, L. (2004). The method Heliosat-2 for deriving shortwave solar radiation from satellite images. *Solar Energy*, *77*, 159−169.

Roebeling, R., Feijt, J., & Stammes, P. (2005). Cloud property retrievals for climate monitoring: Implications of differences between SEVIRI and Meteosat-8 and AVHRR on NOAA-17. *Journal of Geophysical Research*, 111.

Rossow, W., & Garder, L. (1993). Cloud detection using satellite measurements of infrared and visible radiances for ISCCP. *Journal of Climate*, 2341−2369.

Schmetz, J., Pili, Tjemkes, P. S., Just, D., Kerkmann, J., Rota, S., et al. (2002). An introduction to Meteosat Second Generation (MSG). *Bulletin of the American Meteorological Society*, 977−992.

Siegel, D., Westberry, T., & Ohlmann, J. (1999). Cloud color and ocean radiant heating. *Journal of Climate*, *12*, 1101−1116.

Skartveit, A., Olseth, J., & Tuft, M. (1998). An hourly diffuse fraction model with correction for variability and surface albedo. *Solar Energy*, *63*, 173−183.

Suttles, J., & Ohring, G. (1986). Report of the workshop on surface radiation budget for climate applications. *Tech. Rep. WCP-* : World Meteorological Organization 114,144pp.

Van Weele, M., Martin, T., Blumthaler, M., Brogniez, C., den Outer, P., Engelsen, O., et al. (2000). From model intercomparisons towards benchmark UV spectra for six real atmospheric cases. *Journal of Geophysical Research*, *105*, 4915−4925.

Wald, L., Albuisson, M., Best, C., Delamare, C., Dumortier, D., Gaboardi, E., et al. (2002). SoDa: A project for the integration and exploitation of networked solar radiation databases. In W. Pillmann, & K. Tochtermann (Eds.), *Environmental communication in the information society. No. Part 2* (pp. 713−720). Vienna, Austria: International Society for Environmental Protection.

Wang, L., & Qu, J. (2007). NMDI: A normalized multi-band drought index for monitoring soil and vegetation moisture with satellite remote sensing. *Geophysical Research Letters*, 34.

Whitlock, C., Charlock, T., Staylor, W., Pinker, R., Laszlo, I., Ohmury, A., et al. (1995). First global WCRP shortwave surface radiation budget data set. *Bulletin of American Meteorological Society*, 76.

Woick, H., Dewitte, S., Feijt, A., Gratzki, A., Hechler, P., Hollmann, R., et al. (2002). The satellite application facility on climate monitoring. *Advances in Space Research*, *30* (11), 2405−2410.

Wyser, K., O'Hirok, W., & Gautier, C. (2005). A simple method for removing 3-d radiative effects in satellite retrievals of surface irradiance. *Remote Sensing of the Environment*, 94.

Zhang, Y., Rossow, W., & Stackhouse, P. (2007). Comparison of different global information sources used in surface radiative flux calculation: Radiative properties of the surface. *Journal of Geophysical Research*, 112.

Zinner, T., & Mayer, B. (2006). Remote sensing of stratocumulus clouds: Uncertainty and biases due to inhomogeneity. *Journal of Geophysical Research*, 111.